iScience

CellPress
OPEN ACCESS

Article

MiR-4769-3p suppresses adipogenesis in systemic sclerosis by negatively regulating the USP18/VDAC2 pathway

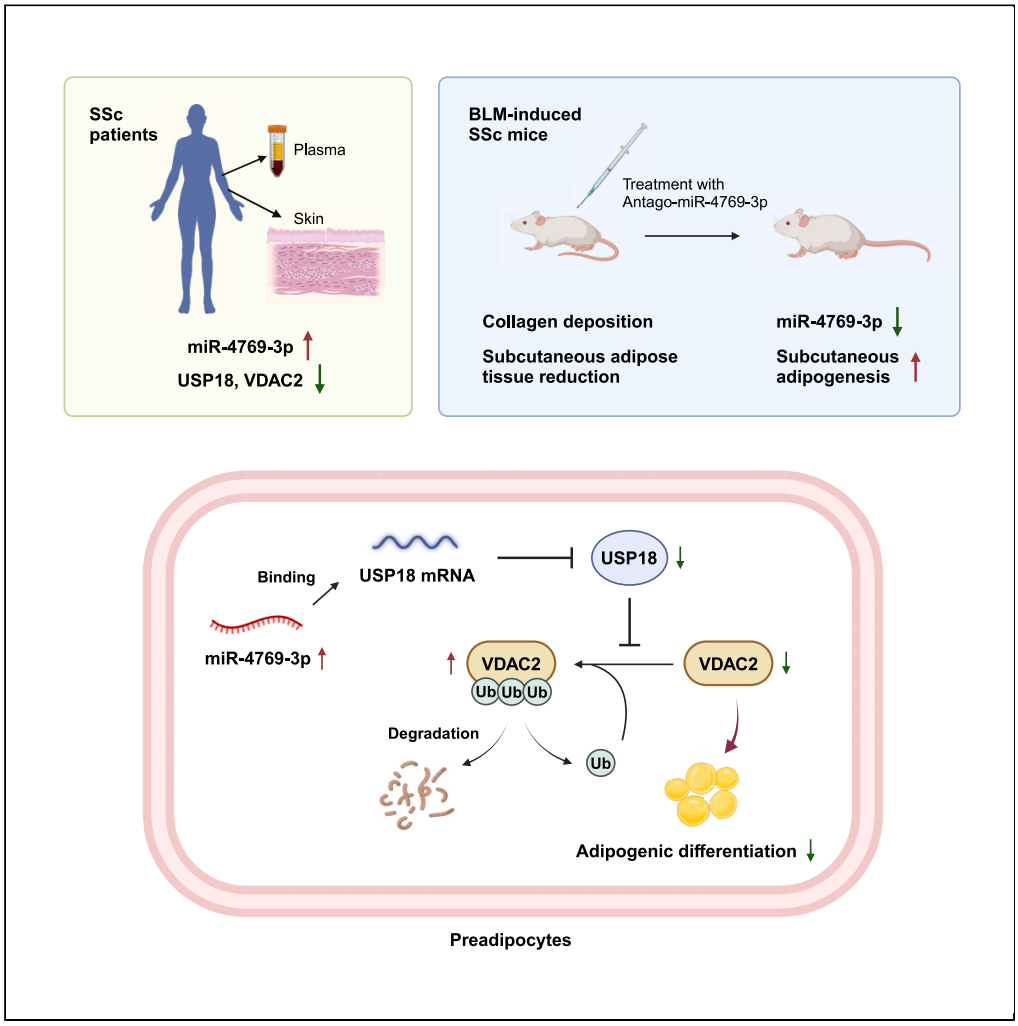

Bingsi Tang, Jiangfan Yu, Rui Tang, ..., Yangfan Xiao, Yan Ding, Rong Xiao

xiaoyangfan@csu.edu.cn (Y.X.)
annymilk@126.com (Y.D.)
xiaorong65@csu.edu.cn (R.X.)

Highlights

MiR-4769-3p was highly expressed in the plasma and skin lesions of SSc patients

MiR-4769-3p silencing ameliorated SSc progression via promoting adipogenesis

MiR-4769-3p negatively regulated USP18 expression to ubiquitinate VDAC2

Elevated miR-4769-3p inhibited the promotion of USP18/VDAC2 axis in adipogenesis

Tang et al., iScience 27, 110483
August 16, 2024
https://doi.org/10.1016/j.isci.2024.110483

iScience

CellPress
OPEN ACCESS

Article

MiR-4769-3p suppresses adipogenesis in systemic sclerosis by negatively regulating the USP18/VDAC2 pathway

Bingsi Tang,[1,2] Jiangfan Yu,[1,2] Rui Tang,[3] Xinglan He,[1,2] Jiani Liu,[1,2] Licong Liu,[1,2] Zehong Song,[1,2] Yaqian Shi,[1,2] Zhuotong Zeng,[1,2] Yi Zhan,[1,2] Xiangning Qiu,[1,2] Yangfan Xiao,[4,5,*] Yan Ding,[6,7,*] and Rong Xiao[1,2,8,*]

SUMMARY

Systemic sclerosis (SSc) is an autoimmune disease affecting multiple tissues. The underlying causes and mechanisms of subcutaneous adipose tissue (SAT) loss in SSc remain unclear. Recent studies have highlighted the role of microRNAs in adipogenesis. Our study found that miR-4769-3p was upregulated in SSc patients and its silencing promoted SAT recovery in bleomycin-induced SSc mice, suggesting that miR-4769-3p might affect adipogenesis in SSc. Manipulating miR-4769-3p expression in 3T3-L1 cells revealed that its inhibition enhanced adipogenesis, while its overexpression weakened it. Further investigations showed that miR-4769-3p bound to 3′UTR of ubiquitin-specific protease-18 (USP18), inhibiting its expression, while USP18 interacted with voltage-dependent anion channel-2 (VDAC2), both of which were reduced in SSc. Silencing either USP18 or VDAC2 attenuated adipogenesis. Notably, USP18 inhibited VDAC2 ubiquitination and degradation, whereas miR-4769-3p reversed the VDAC2-induced elevation of adipogenesis, suggesting that miR-4769-3p inhibited adipogenesis by negatively regulating the USP18/VDAC2 pathway, providing a potential therapeutic target for SSc.

INTRODUCTION

Systemic sclerosis (SSc) is a rare autoimmune connective tissue disease of unclear etiology characterized by immune abnormalities, microangiopathy, and fibrosis.[1–3] SSc is often associated with multiple serious complications, and there are currently no effective treatments, resulting in unmet medical needs that can lead to disability or even death.[1–3]

The pathogenesis of SSc is a complex process that involves communication among multiple cell types. It is widely believed that abnormal fibroblast activation contributes to excessive deposition of collagen and extracellular matrix, which is the main cause of skin fibrosis and abnormal manifestations of internal organs in SSc.[4–6] However, it has been demonstrated that dermal fibrosis in SSc is frequently accompanied by structural destruction of subcutaneous adipose tissue (SAT) and a significant reduction in adipocytes, with fibro-collagen encircling atrophied or destroyed adipocytes.[6–8] The characteristic skin tightness of SSc is thought to be related to the loss of SAT, although the exact mechanism remains to be elucidated.

In recent years, it has become increasingly recognized that adipose tissue homeostasis plays a crucial role in SSc skin fibrosis. As reported, SAT consists of subcutaneous white adipose tissue (SWAT) and dermal white adipose tissue (DWAT), both of which are significantly altered during the disease process of SSc.[7] With the gradual loss of SAT, the structural support and protective role of SWAT are lost, reducing skin fibrotic capacity and exacerbating skin fibrosis in SSc. DWAT is a unique layer of adipose tissue underlying the reticular dermis. Progenitor cells enriched in DWAT can be regulated by peroxisome proliferator-activated receptor-gamma (PPAR-γ) to determine whether to produce adipocytes or dermal reticular fibroblasts.[8,9] Dermal adipocytes (DAs), a highly plastic white adipocyte present in DWAT, can not only differentiate into mature adipocytes to fill SWAT but also undergo adipocyte-to-myofibroblast transformation or secrete anti-fibrotic cytokines to promote dermal fibrosis.[10–13] Recent studies have also shown that autologous adipocyte transplantation contributes to the re-accumulation of DWAT at skin lesions and reduces myofibroblast aggregation, partially reversing SSc skin fibrosis.[7] Therefore, promoting SAT recovery may be an effective treatment strategy for SSc.

[1]Department of Dermatology, The Second Xiangya Hospital of Central South University, Changsha, Hunan 410000, China
[2]Hunan Key Laboratory of Medical Epigenetics, The Second Xiangya Hospital of Central South University, Changsha, Hunan 410000, China
[3]Department of Rheumatology, The Second Xiangya Hospital of Central South University, Changsha, Hunan 410000, China
[4]Clinical Nursing Teaching and Research Section, The Second Xiangya Hospital of Central South University, Changsha, Hunan 410000, China
[5]Department of Anesthesiology, The Second Xiangya Hospital of Central South University, Changsha, Hunan 410000, China
[6]Department of Dermatology, Hainan Provincial Hospital of Skin Disease, Haikou, Hainan 570100, China
[7]Department of Dermatology, Affiliated Dermatology Hospital of Hainan Medical College, Haikou, Hainan 570100, China
[8]Lead contact
*Correspondence: xiaoyangfan@csu.edu.cn (Y.X.), annymilk@126.com (Y.D.), xiaorong65@csu.edu.cn (R.X.)
https://doi.org/10.1016/j.isci.2024.110483

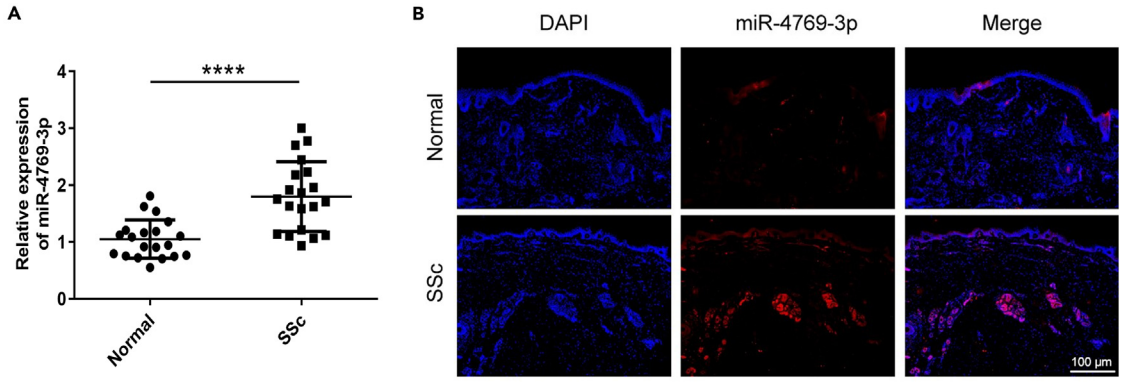

Figure 1. MiR-4769-3p is upregulated in SSc patients

(A) The expression of miR-4769-3p was analyzed using quantitative real-time PCR (real-time qPCR) in plasma samples from 20 SSc patients and 20 healthy controls.

(B) The expression of miR-4769-3p in skin samples from three SSc patients and three healthy controls was assessed by RNA-FISH (blue indicates DAPI, red indicates miR-4769-3p) (100×). Data are presented as mean ± SEM; statistical analysis by Student's t test: ****$p < 0.0001$ versus the healthy control group.

MicroRNAs (miRNAs) are a class of highly stable, noncoding, single-stranded small ribonucleic acids that exist in nearly all body fluids and play powerful regulatory roles in various molecular pathways.[14,15] Notably, dysregulation of several miRNAs involved in fibrosis, immune activation, and vascular changes in SSc has been identified in blood and tissue samples from SSc patients.[16] For example, the expression profiles of circulating free miRNAs were significantly altered in the serum of SSc patients, with downregulation of miR-181a and overexpression of miR-132, -143, -145, and, -155 being the most significant.[17] Also, miR-27a-3p could inhibit lung and skin fibrosis in SSc by negatively regulating SPP1 and extracellular signal-regulated kinase (ERK) signaling.[18] These dysregulated miRNAs could potentially be used as diagnostic and therapeutic targets for SSc.

Recent studies have highlighted that miRNAs play an important role in regulating adipogenesis. For example, miR-144 regulated the C/EBPα–FOXO1 complex to affect adipogenesis in preadipocytes, and miR-424(322)/503 targeted γ-synuclein to regulate adipocyte differentiation and adipose tissue expansion.[19,20] However, the regulatory role of miRNAs in the progressive reduction of SAT in SSc has not been investigated.

Previously, we identified increased expression of miR-4769-3p in the plasma of SSc patients using high-throughput miRNA microarray technology. MiR-4769-3p is a newly discovered miRNA that was only found to be upregulated in psoriasis skin lesions and non-small cell lung cancer serum, downregulated in cervical squamous cell carcinoma tissue, and downregulated in common variant immunodeficiency serum.[21–24] However, its biological function in the aforementioned diseases, including SSc, has not been explored. The aim of this study was to investigate the potential role of miR-4769-3p in the pathogenesis of SSc and its regulatory mechanism in the loss of SAT, providing a new basis for potential intervention targets for SSc treatment.

RESULTS

MiR-4769-3p is upregulated in the plasma and skin lesions of SSc patients

To clarify the differential expression of miR-4769-3p in SSc, we detected plasma samples from 20 SSc patients and 20 healthy controls and found that miR-4769-3p expression was significantly increased in SSc patients (Figure 1A). We then performed RNA fluorescence *in situ* hybridization (RNA-FISH) and observed an increased expression of miR-4769-3p in the cytoplasm of skin lesions collected from SSc patients (Figure 1B). These results indicated that miR-4769-3p was highly expressed in both plasma and skin lesions of SSc patients.

MiR-4769-3p negatively regulates adipogenic differentiation of 3T3-L1 cells

3T3-L1 cells, also known as mouse embryonic fibroblasts or preadipocytes, are the most widely used cell models *in vitro*, so we chose them to investigate the regulatory role of miR-4769-3p in adipogenesis. First, 3T3-L1 cells were cultured in adipogenic differentiation medium for 0, 2, 4, 6, and 8 days and then assayed for miR-4769-3p expression, which showed a gradual decrease of miR-4769-3p over time (Figure 2A). Next, 3T3-L1 cells were transfected with Antago-miR-4769-3p or miR-4769-3p mimics to silence or overexpress miR-4769-3p (Figure 2B), and then these cells were cultured in adipogenic differentiation medium for 8 days before assay. Oil red O staining showed that silencing of miR-4769-3p promoted lipid droplet formation, whereas overexpressing of miR-4769-3p inhibited lipid droplet formation (Figure 2C). Furthermore, the levels of adipogenic proteins (PPAR-γ, FABP4 [fatty acid binding protein-4], SREBP-1 [sterol-regulatory element-binding protein-1], and Lipin1) were increased in miR-4769-3p-silenced cells, whereas they were decreased in miR-4769-3p-overexpressed cells (Figure 2D). These results suggested that miR-4769-3p contributed to the inhibition of adipogenic differentiation of 3T3-L1 cells.

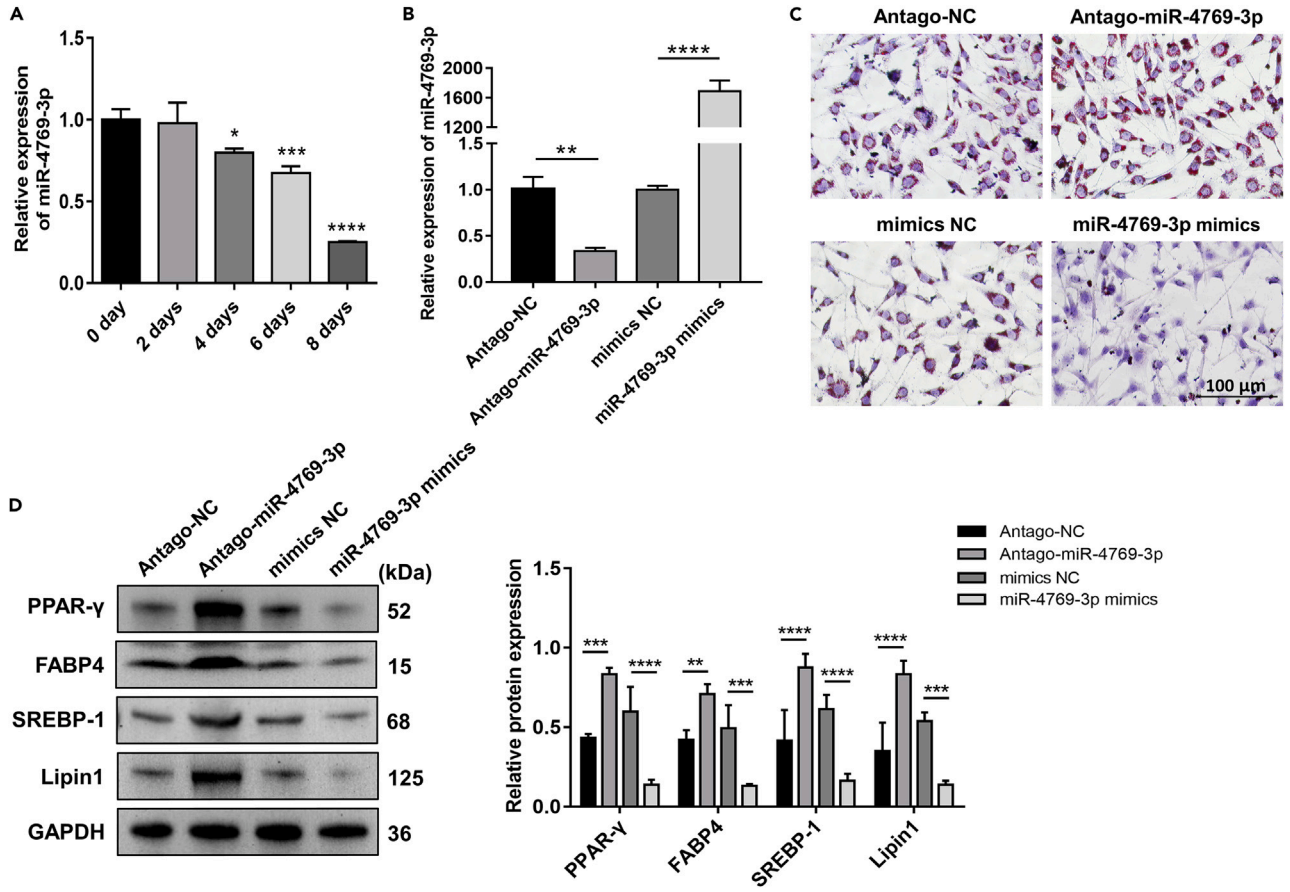

Figure 2. MiR-4769-3p inhibits adipogenic differentiation of 3T3-L1 cells

(A) The expression of miR-4769-3p was analyzed using real-time qPCR in 3T3-L1 cells during adipogenic differentiation for 0, 2, 4, 6, and 8 days.

(B) The expression of miR-4769-3p was analyzed using real-time qPCR in 3T3-L1 cells that were transfected with Antago-miR-4769-3p or miR-4769-3p mimics. (C and D) After inducing adipogenic differentiation in 3T3-L1 cells transfected with Antago-miR-4769-3p or miR-4769-3p mimics for 8 days, lipid droplet formation was assessed using oil red O staining (C) (red indicates stained lipid droplets) (200×), and the levels of adipogenic proteins (PPAR-γ, FABP4, SREBP-1, and Lipin1) were measured using western blot analysis (D). Data are presented as mean ± SEM (n = 3); statistical analysis by ANOVA or Student's t test: *$p < 0.05$, **$p < 0.01$, ***$p < 0.001$, and ****$p < 0.0001$ versus the indicated group.

MiR-4769-3p inhibition promotes adipogenesis in SSc mice

To identify the influences of miR-4769-3p on adipogenesis in SSc *in vivo*, we established a classical mouse model of SSc induced by bleomycin and then injected these mice subcutaneously with Antago-miR-4769-3p or Antago-NC. As assessed by histopathological analysis, bleomycin-injected mice exhibited significant skin thickening, sclerosis, collagen deposition, and SAT reduction compared to sham-operated mice (Figure 3A). Notably, Antago-miR-4769-3p treatment attenuated the aforementioned pathological changes and dramatically promoted adipogenesis in skin tissues of SSc mice, whereas no significant changes were observed in mice treated with Antago-NC (Figure 3A). These changes were also confirmed by oil red O staining (Figure 3A). After Antago-miR-4769-3p treatment, miR-4769-3p expression was decreased (Figure 3B), whereas the levels of adipogenic proteins (PPAR-γ, FABP4, SREBP-1, and Lipin1) were significantly increased (Figure 3C). Overall, inhibition of miR-4769-3p was beneficial in promoting subcutaneous adipogenesis and ameliorating skin fibrosis in SSc mice.

MiR-4769-3p represses adipogenic differentiation by targeting USP18

Since inhibition of miR-4769-3p enhanced subcutaneous adipogenesis in SSc mice, we hoped to explore the potential mechanism of miR-4769-3p in adipogenic differentiation. By searching online databases such as miRWalk for predicted miR-4769-3p targets, we found that miR-4769-3p could bind to the 3′UTR of ubiquitin-specific protease-18 (USP18), a deubiquitinating enzyme that reverses the post-translational regulation of target proteins,[25] thereby inhibiting USP18 expression (Figure 4A). We also found that USP18 was reduced in skin lesions of SSc patients by immunohistochemical staining, which was in contrast to miR-4769-3p (Figure 4B). Next, we induced adipogenic differentiation of 3T3-L1 cells transfected with Antago-miR-4769-3p or miR-4769-3p mimics for 8 days and detected the changes in USP18 expression. The data

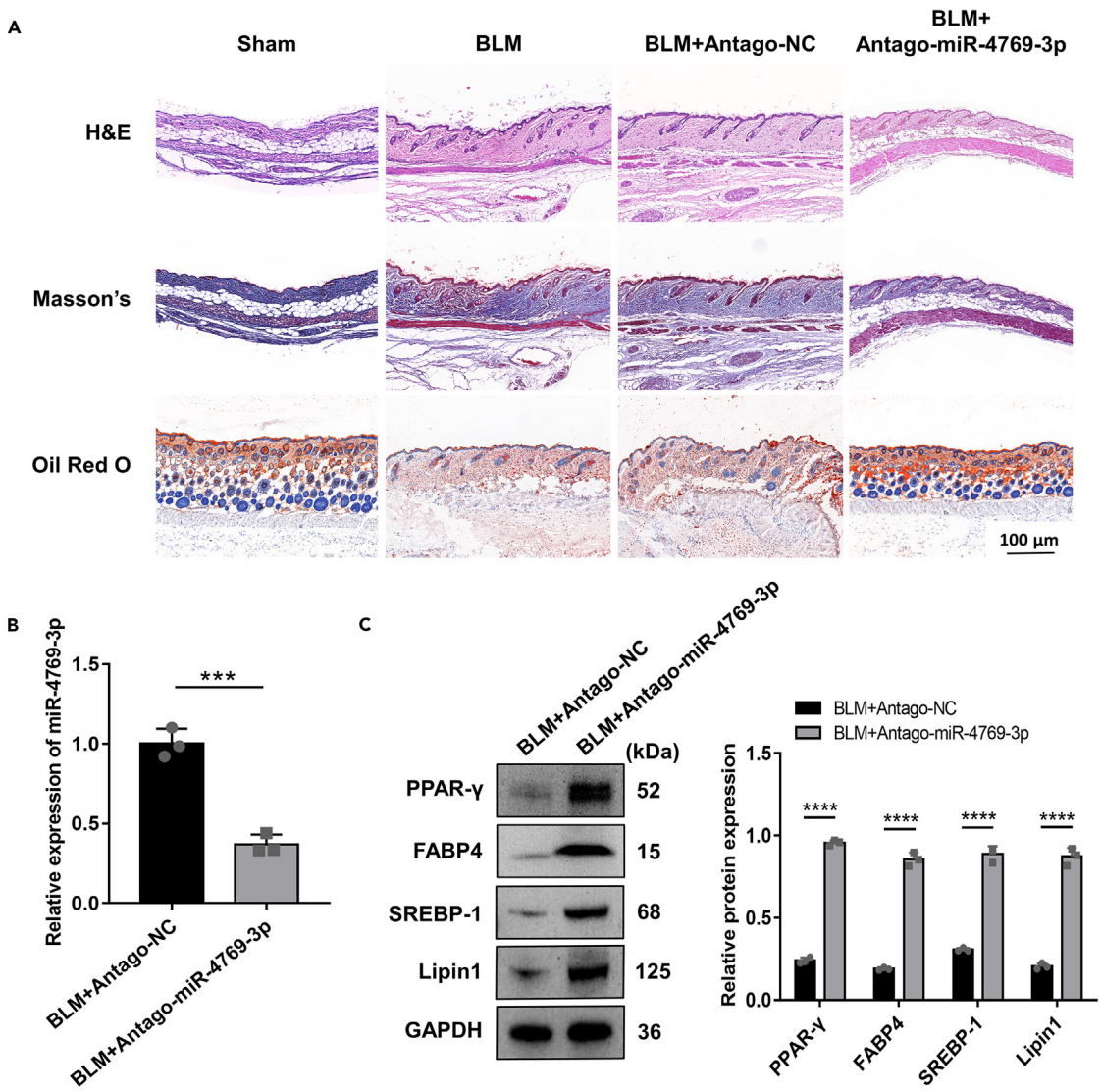

Figure 3. MiR-4769-3p inhibition promotes subcutaneous adipogenesis in SSc mice

The mouse model of SSc was induced with bleomycin and then subcutaneously injected with Antago-miR-4769-3p or Antago-NC.

(A) Histopathological changes in the skin tissues of mice in each group were assessed using H&E and Masson's staining, and subcutaneous adipogenesis was assessed using oil red O staining (red indicates stained lipid droplets) (100×). (B and C) After treatment with Antago-miR-4769-3p or Antago-NC, the expression of miR-4769-3p in skin lesions of bleomycin-induced SSc mice was analyzed using real-time qPCR (B), and the levels of adipogenic proteins (PPAR-γ, FABP4, SREBP-1, and Lipin1) were measured using western blot analysis (C). Data are presented as mean ± SEM (n = 3); statistical analysis by ANOVA or Student's t test: ***$p < 0.001$, and ****$p < 0.0001$ versus the indicated group.

showed that the mRNA and protein levels of USP18 were increased after miR-4769-3p inhibition and decreased after miR-4769-3p overexpression (Figures 4C and 4D). To clarify the interaction between miR-4769-3p and USP18, we performed RNA immunoprecipitation (RIP), which showed that miR-4769-3p and USP18 were enriched in the Ago2 antibody group of 3T3-L1 cells, while it was normal in the input and negative control groups (Figure 4E). Meanwhile, dual luciferase reporter assay indicated that luciferase activity was reduced in the human or mouse USP18 wild-type group and unchanged in the USP18 mutant group after transfection with miR-4769-3p mimics (Figure 4F). All of these data demonstrated a direct interaction between miR-4769-3p and USP18.

Subsequently, we examined the changes of USP18 during adipogenic differentiation of 3T3-L1 cells and found that the mRNA and protein levels of USP18 gradually increased with the prolongation of induction time (Figures 4G and 4H). We then transfected si-USP18 into 3T3-L1 cells and induced adipogenic differentiation for 8 days. In these USP18-silenced cells, lipid droplet formation was significantly inhibited (Figure 4I), and the levels of adipogenic proteins (PPAR-γ, FABP4, SREBP-1, and Lipin1) were significantly decreased (Figure 4J). Taken together, we suggested that miR-4769-3p inhibits adipogenic differentiation of preadipocytes by targeting USP18, thereby exacerbating SAT reduction in SSc.

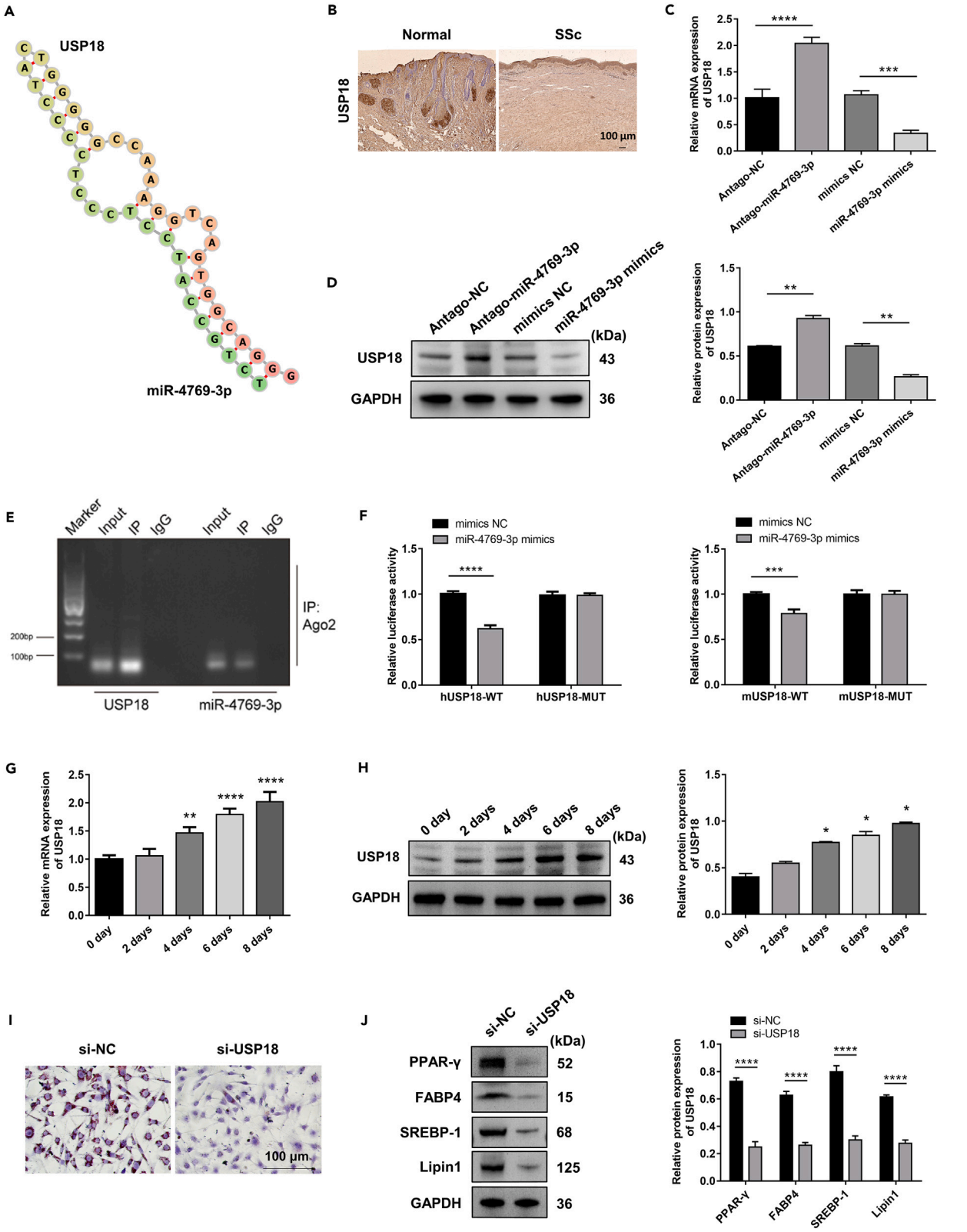
A
USP18
miR-4769-3p
B
Normal
SSc
USP18
100 μm
C
Relative mRNA expression of USP18
Antago-NC
Antago-miR-4769-3p
mimics NC
miR-4769-3p mimics
D
Antago-NC
Antago-miR-4769-3p
mimics NC
miR-4769-3p mimics
(kDa)
USP18
43
GAPDH
36
Relative protein expression of USP18
E
Marker
Input
IP
IgG
200bp
100bp
IP: Ago2
USP18
miR-4769-3p
F
mimics NC
miR-4769-3p mimics
Relative luciferase activity
hUSP18-WT
hUSP18-MUT
mUSP18-WT
mUSP18-MUT
G
Relative mRNA expression of USP18
0 day
2 days
4 days
6 days
8 days
H
(kDa)
USP18
43
GAPDH
36
Relative protein expression of USP18
I
si-NC
si-USP18
100 μm
J
si-NC
si-USP18
(kDa)
PPAR-γ
52
FABP4
15
SREBP-1
68
Lipin1
125
GAPDH
36
Relative protein expression of USP18

Figure 4. USP18, a novel target of miR-4769-3p, promotes adipogenic differentiation of 3T3-L1 cells

(A) The 2D structure of miR-4769-3p bound to the 3′UTR of USP18 was obtained from the miRWalk database.

(B) USP18 expression was evaluated by immunohistochemical staining in skin samples from SSc patients and healthy controls (dark brown indicates USP18) (100×). (C and D) After inducing adipogenic differentiation of 3T3-L1 cells transfected with Antago-miR-4769-3p or miR-4769-3p mimics for 8 days, the mRNA and protein levels of USP18 were analyzed using real-time qPCR (C) and western blot analysis (D), respectively. (E and F) The validation of the direct interaction between miR-4769-3p and USP18 was confirmed through RIP (E) and dual luciferase reporter assay (F).

(G and H) The mRNA and protein levels of USP18 in 3T3-L1 cells during adipogenic differentiation were analyzed using real-time qPCR (G) and western blot analysis (H). (I and J) After inducing adipogenic differentiation of 3T3-L1 cells infected with si-USP18 for 8 days, lipid droplet formation was assessed using oil red O staining (I) (red indicates stained lipid droplets) (200×), and the levels of adipogenic proteins (PPAR-γ, FABP4, SREBP-1, and Lipin1) were measured using western blot analysis (J). Data are presented as mean ± SEM (n = 3); statistical analysis by ANOVA: *$p < 0.05$, **$p < 0.01$, ***$p < 0.001$, and ****$p < 0.0001$ versus the indicated group.

USP18 motivates adipogenesis by suppressing ubiquitination and degradation of VDAC2

To further explore the downstream regulatory mechanisms of USP18, we first transfected the USP18-HA-overexpression (OE) fusion vector into 3T3-L1 cells and validated the overexpression of both USP18 and hemagglutinin (HA) by Western blot (Figure 5A). Next, we evaluated these 3T3-L1 cells co-immunoprecipitated with HA antibody by mass spectrometry (MS) analysis, focusing on voltage-dependent anion channel-2 (VDAC2) (Figure 5B). Using immunohistochemical staining, we found that VDAC2 was reduced in skin lesions of SSc patients, consistent with USP18 (Figure 5C). Subsequently, the interaction between USP18 and VDAC2 was validated by co-immunoprecipitation (coIP) assay (Figure 5D). Furthermore, VDAC2 expression was significantly upregulated after transfection with USP18-HA-OE (Figure 5E), whereas it was significantly downregulated after infection with si-USP18 or si-VDAC2 (Figures 5F and 5G). Functionally, after silencing VDAC2 in 3T3-L1 cells, lipid droplet formation was significantly inhibited (Figure 5H), and the levels of adipogenic proteins (PPAR-γ, FABP4, SREBP-1, and Lipin1) were significantly decreased (Figure 5I). In addition, we measured the ubiquitination level of VDAC2 using a coIP assay and found that the ubiquitin level after IP with VDAC2 was significantly reduced in USP18-overexpressing cells (Figure 5J) but increased in skin lesions of bleomycin-induced SSc mice (Figure 5K). The aforementioned results indicated that USP18 stabilized VDAC2 by inhibiting its ubiquitination and degradation, which in turn synergistically promoted adipogenesis of preadipocytes in SSc.

Abnormal elevation of miR-4769-3p impairs the promotion of VDAC2 in adipogenesis

To investigate the effect of miR-4769-3p on adipogenesis via the USP18/VDAC2 pathway, we induced adipogenic differentiation of 3T3-L1 cells for 8 days after overexpression of miR-4769-3p, VDAC2, or both. We then examined changes in VDAC2 expression and adipogenesis in these cells. The results showed that overexpression of miR-4769-3p significantly decreased the mRNA and protein levels of VDAC2, and simultaneous overexpression of VDAC2 and miR-4769-3p resulted in normalization of VDAC2 expression (Figures 6A and 6B). This suggested that miR-4769-3p could reverse the OE-VDAC2-mediated forced expression of VDAC2, and there is a potential regulatory relationship between miR-4769-3p and VDAC2. Furthermore, these cells showed similar changes in lipid droplet formation and levels of adipogenic proteins (PPAR-γ, FABP4, SREBP-1, and Lipin1), which were increased in VDAC2-overexpressing cells and decreased in miR-4769-3p-overexpressing cells (Figures 6C and 6D). Specifically, miR-4769-3p attenuated the increased adipogenesis induced by VDAC2 overexpression (Figures 6C and 6D). Taken together, miR-4769-3p suppressed the contribution of the USP18/VDAC2 axis to adipogenesis in 3T3-L1 cells.

DISCUSSION

SSc is an incurable autoimmune connective tissue disease of unclear pathogenesis. In previous studies, researchers have observed that, as skin fibrosis progresses in SSc patients and experimentally induced fibrotic mice, the physical structure of SAT is disrupted, and SWAT and DWAT gradually atrophy, disappear, and are eventually replaced by fibrotic tissue.[6,26] There is growing recognition that the progression of skin fibrosis in SSc is closely linked to the loss of SAT, but the specific mechanism of their interaction remains unclear.

In recent years, the role of adipocytes in skin fibrosis has received increasing attention. It has been shown that intradermal adiponectin-positive progenitor cells in DWAT undergo phenotypic transformation from adipocytes to myofibroblasts and that adipose-derived stem cells (ADSCs) in DWAT differentiate into myofibroblasts after bleomycin stimulation.[6,27] In addition, adipocytes could affect themselves and other skin cells through cell-autonomous and paracrine mechanisms. During adipogenic differentiation, DAs release large amounts of PPAR-γ, promoting adipocyte maturation and inhibiting transforming growth factor β (TGF-β)/Smad signaling in fibroblasts, which may have important anti-fibrotic effects in SSc.[28] The combination of PPAR-γ reduction and TGF-β activation may be responsible for the loss of adipocyte status in SSc skin lesions.[29] PPAR-γ treatment improved SAT reduction and dermal fibrosis in SSc.[30] Furthermore, treatment with ADSCs reduced skin fibrosis in SSc mice.[31] Transplantation of adipose-like organs containing mature adipocytes promoted DAs regeneration and reduced dermal fibrosis.[32] In conclusion, adipocytes have a close association with skin fibrosis. Understanding and intervening in the potential mechanisms of adipocyte differentiation may help to improve skin fibrosis in SSc.

Increasing research on miRNAs has revealed that miRNAs play important regulatory roles in adipogenesis. It is noteworthy that miRNAs involved in the regulation of adipogenesis also show abnormalities in SSc. For example, miR-155 expression was shown to be increased in serum and fibroblasts from the dermis and lung of SSc patients, and inhibition of miR-155 could reduce SSc fibrosis.[17,33,34] In addition, miR-155 was found to inhibit adipogenesis by downregulating the expression of the adipogenic transcription factors C/EPBβ, C/EBPα,

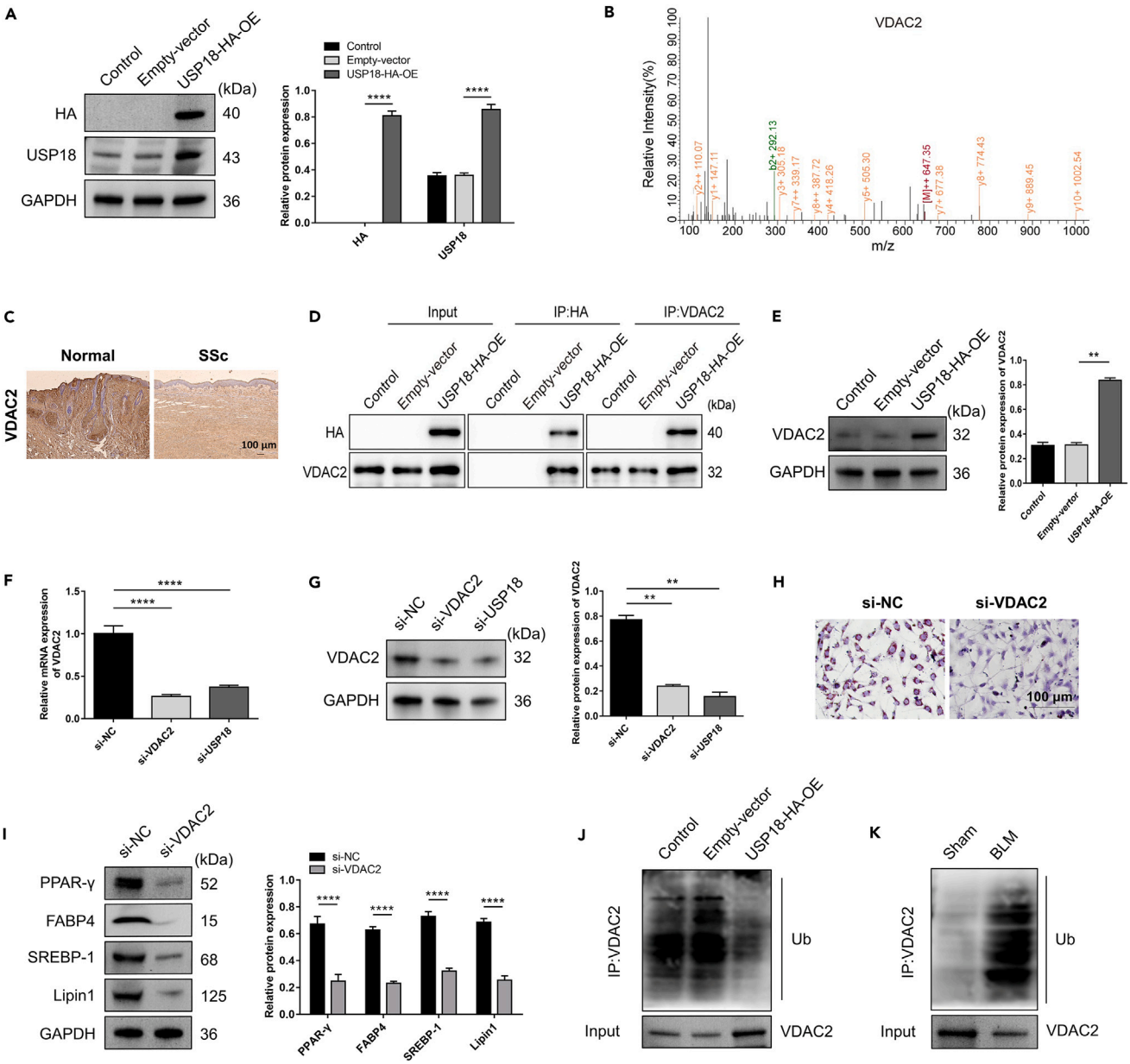

Figure 5. USP18 inhibits the ubiquitination and degradation of VDAC2, synergistically promoting adipogenesis in 3T3-L1 cells

(A) The levels of USP18 and HA in 3T3-L1 cells transfected with USP18-HA-OE fusion vector were measured using western blot analysis.

(B) 3T3-L1 cells co-immunoprecipitated with HA antibody were analyzed by mass spectrometry for the binding proteins of USP18, and finally VDAC2 was focalized.

(C) VDAC2 expression was evaluated by immunohistochemical staining in skin samples from SSc patients and healthy controls (dark brown indicates VDAC2) (100×).

(D) 3T3-L1 cells co-immunoprecipitated with HA or VDAC2 antibodies were analyzed by coIP assay to verify the direct binding between USP18 and VDAC2.

(E) VDAC2 expression in 3T3-L1 cells transfected with USP18-HA-OE fusion vector were measured using western blot analysis. (F and G) The mRNA and protein levels of VDAC2 in 3T3-L1 cells infected with si-USP18 or si-VDAC2 were analyzed using real-time qPCR (F) and western blot analysis (G). (H and I) After inducing adipogenic differentiation of 3T3-L1 cells infected with si-VDAC2 for 8 days, lipid droplet formation was assessed using oil red O staining (H) (red indicates stained lipid droplets) (200×), and the levels of adipogenic proteins (PPAR-γ, FABP4, SREBP-1, and Lipin1) were measured using western blot analysis (I).

(J and K) The ubiquitination level of VDAC2 was analyzed by coIP assay in USP18-overexpressing cells (J) or skin lesions of bleomycin-induced SSc mice (K) after immunoprecipitation with VDAC2. Data are presented as mean ± SEM (n = 3); statistical analysis by ANOVA or Student's t test: $^{**}p < 0.01$ and $^{****}p < 0.0001$ versus the indicated group.

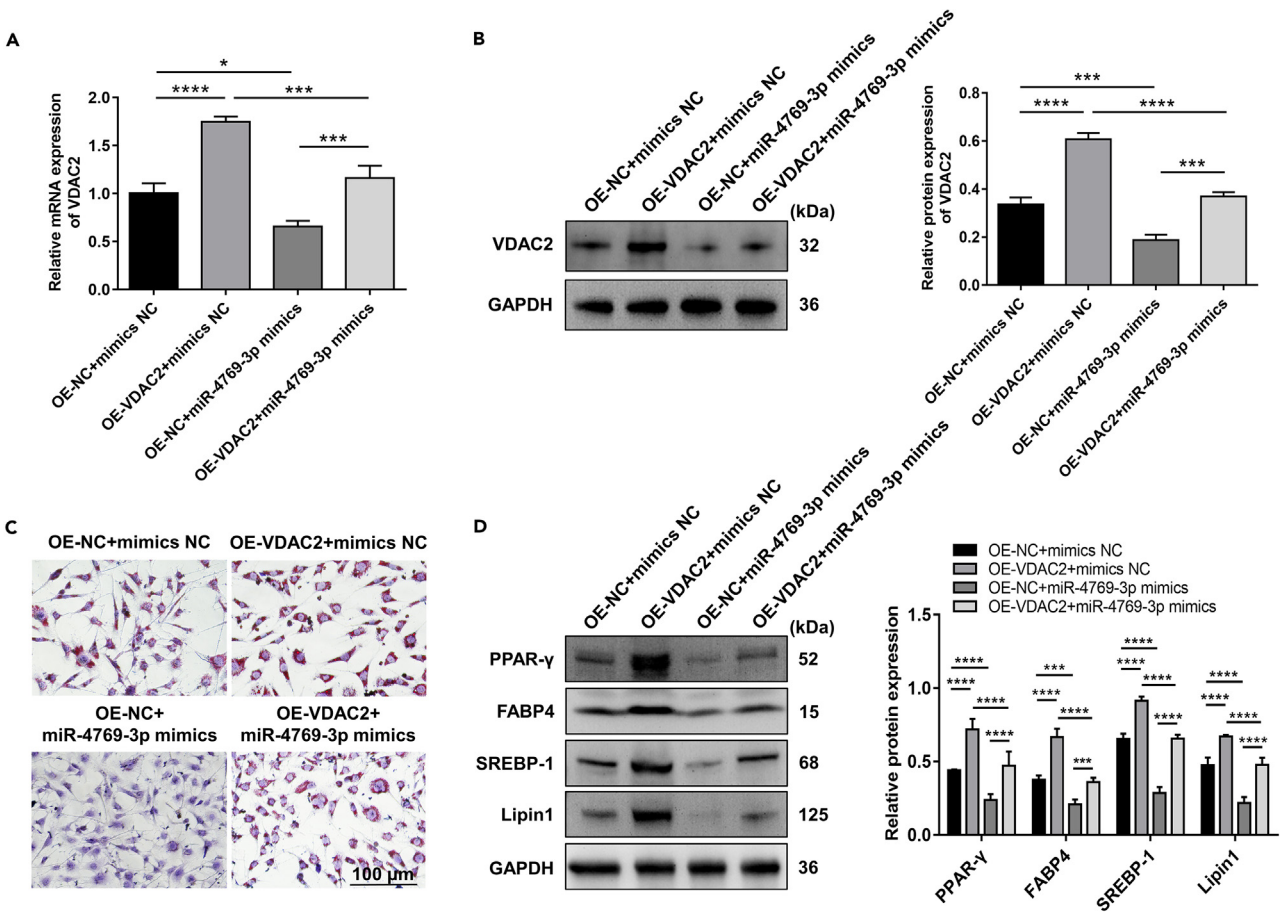

Figure 6. Overexpression of miR-4769-3p abolished USP18/VDAC2-mediated adipogenesis

After transfection with miR-4769-3p mimics, OE-VDAC2, or both, 3T3-L1 cells were induced to undergo adipogenic differentiation for 8 days. (A and B) The mRNA and protein levels of VDAC2 in these cells were analyzed using real-time qPCR (A) and western blot analysis (B).

(C) The lipid droplet formation was assessed using oil red O staining (red indicates stained lipid droplets) (200×).

(D) The levels of adipogenic proteins (PPAR-γ, FABP4, SREBP-1, and Lipin1) were measured using western blot analysis. Data are presented as mean ± SEM (n = 3); statistical analysis by ANOVA: *$p < 0.05$, ***$p < 0.001$, and ****$p < 0.0001$ versus the indicated group.

and PPAR-γ.[35,36] However, the regulatory role of these miRNAs in reducing SAT during SSc progression has not been investigated and the mechanism remains unknown.

In this study, we found that miR-4769-3p was abnormally highly expressed in both plasma and skin lesions of SSc patients, but its biological role in SSc and its regulatory mechanism in adipogenesis are still unclear. By studying adipogenic differentiation in 3T3-L1 cells, it was observed that miR-4769-3p expression gradually decreased as adipogenic differentiation progressed. The lipid droplet formation and the levels of adipogenic proteins were enhanced by inhibition of miR-4769-3p, while overexpression of miR-4769-3p attenuated them. We further investigated the role of miR-4769-3p in bleomycin-induced SSc mice and found that inhibition of miR-4769-3p ameliorated the loss of SAT and increased adipogenic protein levels in skin lesions. These results suggest that miR-4769-3p plays a role in inhibiting adipogenesis in SSc, but the mechanism requires further clarification.

To investigate the potential mechanism by which miR-4769-3p regulates adipogenesis, we searched online databases such as miRWalk for predicted miR-4769-3p targets and found that miR-4769-3p could bind to the 3'UTR of USP18. USP18 is a deubiquitinase that plays a critical role in several pathophysiological processes, including tumorigenesis, inflammation, and mitochondrial autophagy.[37] Functionally, USP18 removed ubiquitin or ISG15 from conjugated proteins in an uncoupling activity-dependent manner and negatively regulated type I interferon (IFN) signaling.[25] USP18 was reported to regulate the stability of FOXO3a by de-ISGylation, thereby reducing TGF-β1-induced fibronectin expression in human lung fibroblasts, suggesting its potential regulatory role in TGF-β1-mediated fibrotic diseases.[38] In addition, USP18 regulated regulatory T (Treg) cell differentiation and affected peripheral T cell homeostasis, suggesting that it may be a promising target for the treatment of various autoimmune diseases.[39] Notably, USP18 also regulated lipid and fatty acid metabolism. Overexpression of USP18 in lung cancer cells upregulated adipose triglyceride lipase expression and enhanced uncoupling protein-1 by decreasing ubiquitination, thereby increasing cellular fatty acid β-oxidation.[40] Based on the close association of USP18 with

differentiation and lipid metabolism, as well as its potential role in fibrosis and autoimmune diseases, it is hypothesized that USP18 may play a role in the development of SSc.

Interestingly, our study showed that USP18 expression was downregulated in skin samples from SSc patients. It was significantly decreased by miR-4769-3p overexpression but increased by miR-4769-3p inhibition. The interaction between miR-4769-3p and USP18 was confirmed by RIP and dual luciferase reporter assay. Furthermore, USP18 expression gradually increased with the progression of adipogenic differentiation of 3T3-L1 cells. The lipid droplet formation and adipogenic protein expression were reduced in USP18-silenced cells. These results suggested that miR-4769-3p could inhibit the adipogenic differentiation of preadipocytes by targeting USP18, thereby promoting the development of SSc.

To further elucidate how USP18 regulates adipocyte differentiation, we identified VDAC2 as a potential USP18-interacting protein by coIP/MS analysis. VDAC2 is a mitochondrial outer membrane protein that regulates Ca^{2+} homeostasis, mitochondrial autophagy, apoptosis, and iron death.[41–43] It has been shown that mitochondrial damage progressively accumulates in TGF-β-exposed fibroblasts and promotes transcriptional regulation of fibroblast activation and fibrosis-associated genes, thereby accelerating SSc progression.[44] In addition, VDAC2 has been implicated in controlling the processing and activity of steroidogenic acute regulatory proteins, which regulate steroidogenesis.[45] Interestingly, in the absence of VDAC2, the adipogenic differentiation of 3T3-L1 cells was significantly inhibited.[46] This is consistent with our findings that VDAC2 silencing decreased lipid droplet formation and adipogenic protein expression in 3T3-L1 cells, whereas overexpressing VDAC2 enhanced their adipogenic differentiation. Our study also found that VDAC2 expression was reduced in skin samples from SSc patients. And it was increased in USP18-overexpressing cells but decreased in USP18-silencing cells. Furthermore, the ubiquitination level of VDAC2 was significantly reduced in USP18-overexpressing cells, while it was significantly increased in skin lesions of bleomycin-induced SSc mice. And miR-4769-3p could reverse the increased adipogenesis induced by VDAC2 overexpression. Taken together, miR-4769-3p could inhibit adipocyte differentiation in SSc by suppressing VDAC2 expression through inhibiting USP18-mediated deubiquitination.

MiR-4769-3p is a newly discovered miRNA that has not been previously studied in relation to SSc or adipogenic metabolism. Our study provides the initial evidence that miR-4769-3p may contribute to the loss of SAT in SSc by inhibiting the adipogenic differentiation of preadipocytes and elucidates the regulatory role of the miR-4769-3p/USP18/VDAC2 axis in adipogenesis. Although previous studies have shown that USP18 functions in the regulation of lipid and fatty acid metabolism, the mechanism by which USP18 regulates adipogenesis remains unclear.[40] Our study showed that USP18 could promote adipogenic differentiation of preadipocytes by mediating the ubiquitination and degradation of VDAC2, and miR-4769-3p inhibited this process by targeting USP18. These findings have translational implications. Targeting miR-4769-3p or USP18 may help to treat diseases with impaired adipogenesis such as SSc.

In conclusion, our results indicated that miR-4769-3p could inhibit adipogenesis by suppressing USP18 expression and USP18-mediated deubiquitination, which leads to the ubiquitination and degradation of VDAC2, ultimately resulting in the loss of SAT in SSc. Our study provides a potential interventional target and additional therapeutic options for SSc.

Limitations of the study

In the development of SSc, miR-4769-3p may play a complicated role. Our study was limited to experimentally confirming the role of miR-4769-3p in promoting SAT loss by inhibiting adipocyte differentiation. The potential of miR-4769-3p to promote the metamorphosis of preadipocytes into myofibroblasts remains to be investigated. Furthermore, our study validated the effects of USP18 and VDAC2, the downstream genes of miR-4769-3p, on adipogenesis only in 3T3-L1 cells, and further validation of these findings in transgenic mice overexpressing USP18 or VDAC2 is needed. Finally, given that the SSc patients included in our study were initially diagnosed at our institution without systemic treatment, our clinical sample size was relatively small and required expansion for extended analysis.

STAR★METHODS

Detailed methods are provided in the online version of this paper and include the following:

- KEY RESOURCES TABLE
- RESOURCE AVAILABILITY
  - Lead contact
  - Materials availability
  - Data and code availability
- EXPERIMENTAL MODEL AND STUDY PARTICIPANT DETAILS
  - Clinical samples
  - Cell culture and induction of adipocyte differentiation
  - Animal model
- METHOD DETAILS
  - RNA fluorescence *in situ* hybridization (RNA-FISH)
  - Hematoxylin–Eosin and Masson's staining
  - Immunohistochemical staining
  - Cell transfection and lentivirus infection
  - Quantitative real-time polymerase chain reaction (real-time qPCR)

- Oil Red O staining
- RNA immunoprecipitation (RIP)
- Dual Luciferase reporter assay
- Co-immunoprecipitation and mass spectrometry (coIP/MS)
- Western blot

- QUANTIFICATION AND STATISTICAL ANALYSIS

ACKNOWLEDGMENTS

Thanks to LetPub (www.letpub.com) for its language help during the preparation of this manuscript. This work was supported by grants from the National Natural Science Foundation of China (no. 82373486, 82073449, 81773333, 82203932, 82203930, and 82001738).

AUTHOR CONTRIBUTIONS

B.T.: conceptualization, data curation, formal analysis, visualization, writing – original draft, and writing – review and editing. J.Y.: data curation and formal analysis. R.T.: data curation and funding acquisition. X.H., J.L., L.L., and Z.S.: data curation. Z.Z., Y.Z., and X.Q.: conceptualization and supervision. Y.S. and Y.X.: writing – review and editing and funding acquisition. Y.D.: writing – review and editing and supervision. R.X.: conceptualization, writing – review and editing, funding acquisition, supervision, and project administration. All authors critically revised the manuscript and provided their comments.

DECLARATION OF INTERESTS

The authors declare no competing interests.

Received: October 14, 2023
Revised: March 29, 2024
Accepted: July 8, 2024
Published: July 10, 2024

REFERENCES

1. Xue, E., Minniti, A., Alexander, T., Del Papa, N., and Greco, R.; On Behalf Of The Autoimmune Diseases Working Party Adwp Of The European Society For Blood; Marrow Transplantation Ebmt (2022). Cellular-Based Therapies in Systemic Sclerosis: From Hematopoietic Stem Cell Transplant to Innovative Approaches. Cells *11*, 3346. https://doi.org/10.3390/cells11213346.
2. Shi, Y., Xiao, Y., Yu, J., Liu, J., Liu, L., Ding, Y., Qiu, X., Zhan, Y., Tang, R., Zeng, Z., and Xiao, R. (2023). UVA1 irradiation attenuates collagen production via Ficz/AhR/MAPK signaling activation in scleroderma. Int. Immunopharmacol. *116*, 109764. https://doi.org/10.1016/j.intimp.2023.109764.
3. O'Reilly, S. (2024). Emerging therapeutic targets in systemic sclerosis. J. Mol. Med. *102*, 465–478. https://doi.org/10.1007/s00109-024-02424-w.
4. Abraham, D., Lescoat, A., and Stratton, R. (2024). Emerging diagnostic and therapeutic challenges for skin fibrosis in systemic sclerosis. Mol. Aspects Med. *96*, 101252. https://doi.org/10.1016/j.mam.2024.101252.
5. Kanno, Y. (2023). The uPA/uPAR System Orchestrates the Inflammatory Response, Vascular Homeostasis, and Immune System in Fibrosis Progression. Int. J. Mol. Sci. *24*, 1796. https://doi.org/10.3390/ijms24021796.
6. Marangoni, R.G., Korman, B.D., Wei, J., Wood, T.A., Graham, L.V., Whitfield, M.L., Scherer, P.E., Tourtellotte, W.G., and Varga, J. (2015). Myofibroblasts in murine cutaneous fibrosis originate from adiponectin-positive intradermal progenitors. Arthritis Rheumatol. *67*, 1062–1073. https://doi.org/10.1002/art.38990.
7. Wang, J., Cai, J., Zhang, Q., Wen, J., Liao, Y., and Lu, F. (2022). Fat transplantation induces dermal adipose regeneration and reverses skin fibrosis through dedifferentiation and redifferentiation of adipocytes. Stem Cell Res. Ther. *13*, 499. https://doi.org/10.1186/s13287-022-03127-0.
8. Varga, J., and Marangoni, R.G. (2017). Systemic sclerosis in 2016: Dermal white adipose tissue implicated in SSc pathogenesis. Nat. Rev. Rheumatol. *13*, 71–72. https://doi.org/10.1038/nrrheum.2016.223.
9. Driskell, R.R., Jahoda, C.A., Chuong, C.M., Watt, F.M., and Horsley, V. (2014). Defining dermal adipose tissue. Exp. Dermatol. *23*, 629–631. https://doi.org/10.1111/exd.12450.
10. Chen, S.X., Zhang, L.J., and Gallo, R.L. (2019). Dermal White Adipose Tissue: A Newly Recognized Layer of Skin Innate Defense. J. Invest. Dermatol. *139*, 1002–1009. https://doi.org/10.1016/j.jid.2018.12.031.
11. Zhang, Z., Shao, M., Hepler, C., Zi, Z., Zhao, S., An, Y.A., Zhu, Y., Ghaben, A.L., Wang, M.Y., Li, N., et al. (2019). Dermal adipose tissue has high plasticity and undergoes reversible dedifferentiation in mice. J. Clin. Invest. *129*, 5327–5342. https://doi.org/10.1172/JCI130239.
12. Kruglikov, I.L., and Scherer, P.E. (2016). Dermal Adipocytes: From Irrelevance to Metabolic Targets? Trends Endocrinol. Metab. *27*, 1–10. https://doi.org/10.1016/j.tem.2015.11.002.
13. Liu, S.Y., Wu, J.J., Chen, Z.H., Zou, M.L., Teng, Y.Y., Zhang, K.W., Li, Y.Y., Guo, D.Y., Yuan, F.L., and Li, X. (2022). Insight into the role of dermal white adipose tissue loss in dermal fibrosis. J. Cell. Physiol. *237*, 169–177. https://doi.org/10.1002/jcp.30552.
14. Szabo, I., Muntean, L., Crisan, T., Rednic, V., Sirbe, C., and Rednic, S. (2021). Novel Concepts in Systemic Sclerosis Pathogenesis: Role for miRNAs. Biomedicines *9*, 1471. https://doi.org/10.3390/biomedicines9101471.
15. Bayati, P., Kalantari, M., Assarehzadegan, M.A., Poormoghim, H., and Mojtabavi, N. (2022). MiR-27a as a diagnostic biomarker and potential therapeutic target in systemic sclerosis. Sci. Rep. *12*, 18932. https://doi.org/10.1038/s41598-022-23723-7.
16. Liu, Y., Cheng, L., Zhan, H., Li, H., Li, X., Huang, Y., and Li, Y. (2022). The Roles of Noncoding RNAs in Systemic Sclerosis. Front. Immunol. *13*, 856036. https://doi.org/10.3389/fimmu.2022.856036.
17. Wajda, A., Walczyk, M., Dudek, E., Stypinska, B., Lewandowska, A., Romanowska-Prochnicka, K., Chojnowski, M., Olesinska, M., and Paradowska-Gorycka, A. (2022). Serum microRNAs in Systemic Sclerosis, Associations with Digital Vasculopathy and Lung Involvement. Int. J. Mol. Sci. *23*, 10731. https://doi.org/10.3390/ijms231810731.
18. Cheng, Q., Chen, M., Wang, H., Chen, X., Wu, H., Du, Y., and Xue, J. (2022). MicroRNA-27a-3p inhibits lung and skin fibrosis of systemic sclerosis by negatively regulating SPP1. Genomics *114*, 110391. https://doi.org/10.1016/j.ygeno.2022.110391.
19. Rodriguez-Barrueco, R., Latorre, J., Devis-Jauregui, L., Lluch, A., Bonifaci, N., Llobet, F.J., Olivan, M., Coll-Iglesias, L., Gassner, K., Davis, M.L., et al. (2022). A microRNA Cluster Controls Fat Cell Differentiation and Adipose Tissue Expansion By Regulating SNCG. Adv.

Sci. *9*, e2104759. https://doi.org/10.1002/advs.202104759.
20. Lin, W., Wen, X., Li, X., Chen, L., Wei, W., Zhang, L., and Chen, J. (2022). MiR-144 regulates adipogenesis by mediating formation of C/EBPα-FOXO1 protein complex. Biochem. Biophys. Res. Commun. *612*, 126–133. https://doi.org/10.1016/j.bbrc.2022.04.093.
21. De Felice, B., Nigro, E., Polito, R., Rossi, F.W., Pecoraro, A., Spadaro, G., and Daniele, A. (2020). Differently expressed microRNA in response to the first Ig replacement therapy in common variable immunodeficiency patients. Sci. Rep. *10*, 21482. https://doi.org/10.1038/s41598-020-77100-3.
22. Qiao, M., Ding, J., Yan, J., Li, R., Jiao, J., and Sun, Q. (2018). Circular RNA Expression Profile and Analysis of Their Potential Function in Psoriasis. Cell. Physiol. Biochem. *50*, 15–27. https://doi.org/10.1159/000493952.
23. Zhang, X., Tan, J., Chen, Y., Ma, S., Bai, W., Peng, Y., and Shi, G. (2022). Identification of serum MiRNAs as candidate biomarkers for non-small cell lung cancer diagnosis. BMC Pulm. Med. *22*, 479. https://doi.org/10.1186/s12890-022-02267-6.
24. Kwon, A.Y., Jeong, J.Y., Park, H., Hwang, S., Kim, G., Kang, H., Heo, J.H., Lee, H.J., Kim, T.H., and An, H.J. (2022). miR-22-3p and miR-30e-5p Are Associated with Prognosis in Cervical Squamous Cell Carcinoma. Int. J. Mol. Sci. *23*, 5623. https://doi.org/10.3390/ijms23105623.
25. Kang, J.A., and Jeon, Y.J. (2020). Emerging Roles of USP18: From Biology to Pathophysiology. Int. J. Mol. Sci. *21*, 6825. https://doi.org/10.3390/ijms21186825.
26. Marangoni, R.G., and Lu, T.T. (2017). The roles of dermal white adipose tissue loss in scleroderma skin fibrosis. Curr. Opin. Rheumatol. *29*, 585–590. https://doi.org/10.1097/BOR.0000000000000437.
27. Ohgo, S., Hasegawa, S., Hasebe, Y., Mizutani, H., Nakata, S., and Akamatsu, H. (2013). Bleomycin inhibits adipogenesis and accelerates fibrosis in the subcutaneous adipose layer through TGF-β1. Exp. Dermatol. *22*, 769–771. https://doi.org/10.1111/exd.12256.
28. Korman, B., Marangoni, R.G., Lord, G., Olefsky, J., Tourtellotte, W., and Varga, J. (2018). Adipocyte-specific Repression of PPAR-gamma by NCoR Contributes to Scleroderma Skin Fibrosis. Arthritis Res. Ther. *20*, 145. https://doi.org/10.1186/s13075-018-1630-z.
29. Taylor, B., Shah, A., and Bielczyk-Maczynska, E. (2020). TGF-β is insufficient to induce adipocyte state loss without concurrent PPARγ downregulation. Sci. Rep. *10*, 14084. https://doi.org/10.1038/s41598-020-71100-z.
30. Ghosh, A.K. (2021). Pharmacological activation of PPAR-γ: a potential therapy for skin fibrosis. Int. J. Dermatol. *60*, 376–383. https://doi.org/10.1111/ijd.15388.
31. Wang, H.C., Sun, E.T., Zhao, R.C., Chen, B., Han, Q., Li, N., Long, X., and Wang, X. (2023). Adipose-Derived Stem Cells Attenuate Skin Fibrosis and Improve Fat Retention of a Localized Scleroderma Mouse Model. Plast. Reconstr. Surg. *151*, 97–107. https://doi.org/10.1097/PRS.0000000000009796.
32. Quan, Y.P., Zhang, Y.T., Li, J., Lu, F., and Cai, J.R. (2023). Transplantation of in vitro prefabricated adipose organoids attenuates skin fibrosis by restoring subcutaneous fat and inducing dermal adipogenesis. Faseb. J. *37*, e23076. https://doi.org/10.1096/fj.202202117R.
33. Henry, T.W., Mendoza, F.A., and Jimenez, S.A. (2019). Role of microRNA in the pathogenesis of systemic sclerosis tissue fibrosis and vasculopathy. Autoimmun. Rev. *18*, 102396. https://doi.org/10.1016/j.autrev.2019.102396.
34. Artlett, C.M., Sassi-Gaha, S., Hope, J.L., Feghali-Bostwick, C.A., and Katsikis, P.D. (2017). Mir-155 is overexpressed in systemic sclerosis fibroblasts and is required for NLRP3 inflammasome-mediated collagen synthesis during fibrosis. Arthritis Res. Ther. *19*, 144. https://doi.org/10.1186/s13075-017-1331-z.
35. Liu, Y., Wang, M., Deng, T., Liu, R., Ning, T., Bai, M., Ying, G., Zhang, H., and Ba, Y. (2022). Exosomal miR-155 from gastric cancer induces cancer-associated cachexia by suppressing adipogenesis and promoting brown adipose differentiation *via* C/EPBbeta. Cancer Biol. Med. *19*, 1301–1314. https://doi.org/10.20892/j.issn.2095-3941.2021.0220.
36. Yu, Z., Luo, R., Li, Y., Li, X., Yang, Z., Peng, J., and Huang, K. (2022). ADAR1 inhibits adipogenesis and obesity by interacting with Dicer to promote the maturation of miR-155-5P. J. Cell Sci. *135*, jcs259333. https://doi.org/10.1242/jcs.259333.
37. Song, M.Y., Yi, F., Zeng, F.Y., Zheng, L., Huang, L., Sun, X.Y., Huang, Q.Y., Deng, J., Wang, H., and Gu, W.P. (2024). USP18 Stabilized FTO Protein to Activate Mitophagy in Ischemic Stroke Through Repressing m6A Modification of SIRT6. Mol. Neurobiol. https://doi.org/10.1007/s12035-024-04001-1.
38. Wang, B., Li, Y., Wang, H., Zhao, J., Zhao, Y., Liu, Z., and Ma, H. (2020). FOXO3a is stabilized by USP18-mediated de-ISGylation and inhibits TGF-β1-induced fibronectin expression. J. Investig. Med. *68*, 786–791. https://doi.org/10.1136/jim-2019-001145.
39. Yang, L., Jing, Y., Kang, D., Jiang, P., Li, N., Zhou, X., Chen, Y., Westerberg, L.S., and Liu, C. (2021). Ubiquitin-specific peptidase 18 regulates the differentiation and function of Treg cells. Genes Dis. *8*, 344–352. https://doi.org/10.1016/j.gendis.2020.03.004.
40. Liu, X., Lu, Y., Chen, Z., Liu, X., Hu, W., Zheng, L., Chen, Y., Kurie, J.M., Shi, M., Mustachio, L.M., et al. (2021). The Ubiquitin-Specific Peptidase USP18 Promotes Lipolysis, Fatty Acid Oxidation, and Lung Cancer Growth. Mol. Cancer Res. *19*, 667–677. https://doi.org/10.1158/1541-7786.MCR-20-0579.
41. Shankar, T.S., Ramadurai, D.K.A., Steinhorst, K., Sommakia, S., Badolia, R., Thodou Krokidi, A., Calder, D., Navankasattusas, S., Sander, P., Kwon, O.S., et al. (2021). Cardiac-specific deletion of voltage dependent anion channel 2 leads to dilated cardiomyopathy by altering calcium homeostasis. Nat. Commun. *12*, 4583. https://doi.org/10.1038/s41467-021-24869-0.
42. Yi, K.Z., Liu, J.C., Rong, Y., Wang, C., Tang, X., Zhang, X.P., Xiong, Y.H., and Wang, F.B. (2021). Biological Functions and Prognostic Value of Ferroptosis-Related Genes in Bladder Cancer. Front. Mol. Biosci. *8*, 631152. https://doi.org/10.3389/fmolb.2021.631152.
43. Koushi, M., Aoyama, Y., Kamei, Y., and Asakai, R. (2020). Bisindolylpyrrole triggers transient mitochondrial permeability transitions to cause apoptosis in a VDAC1/2 and cyclophilin D-dependent manner via the ANT-associated pore. Sci. Rep. *10*, 16751. https://doi.org/10.1038/s41598-020-73667-z.
44. Zhou, X., Trinh-Minh, T., Tran-Manh, C., Giessl, A., Bergmann, C., Gyorfi, A.H., Schett, G., and Distler, J.H.W. (2022). Impaired Mitochondrial Transcription Factor A Expression Promotes Mitochondrial Damage to Drive Fibroblast Activation and Fibrosis in Systemic Sclerosis. Arthritis Rheumatol. *74*, 871–881. https://doi.org/10.1002/art.42033.
45. Prasad, M., Kaur, J., Pawlak, K.J., Bose, M., Whittal, R.M., and Bose, H.S. (2015). Mitochondria-associated Endoplasmic Reticulum Membrane (MAM) Regulates Steroidogenic Activity via Steroidogenic Acute Regulatory Protein (StAR)-Voltage-dependent Anion Channel 2 (VDAC2) Interaction. J. Biol. Chem. *290*, 2604–2616. https://doi.org/10.1074/jbc.M114.605808.
46. Ye, F., Zhang, H., Yang, Y.X., Hu, H.D., Sze, S.K., Meng, W., Qian, J., Ren, H., Yang, B.L., Luo, M.Y., et al. (2011). Comparative proteome analysis of 3T3-L1 adipocyte differentiation using iTRAQ-coupled 2D LC-MS/MS. J. Cell. Biochem. *112*, 3002–3014. https://doi.org/10.1002/jcb.23223.

STAR★METHODS

KEY RESOURCES TABLE

REAGENT or RESOURCE	SOURCE	IDENTIFIER
Antibodies		
Anti-PPAR delta antibody	Abcam	Cat# ab178866; RRID: AB_2722649
Anti-FABP4 antibody	Abcam	Cat# ab92501; RRID: AB_10562486
Anti-SREBP1 antibody	Abcam	Cat# ab28481; RRID: AB_778069
Anti-Lipin1 antibody	Abcam	Cat# ab181389
Anti-GAPDH antibody	Abcam	Cat# ab9485; RRID: AB_307275
Anti-Argonaute-2 antibody	Abcam	Cat# ab156870; RRID: AB_2687492
USP18 Polyclonal antibody	Proteintech	Cat# 12153-1-AP; RRID: AB_2877830
VDAC2 Polyclonal antibody	Proteintech	Cat# 11663-1-AP; RRID: AB_2304144
HA tag Polyclonal antibody	Proteintech	Cat# 51064-2-AP; RRID: AB_11042321
Ubiquitin (P4D1) Mouse mAb	Cell Signaling Technology	Cat# 3936; RRID: AB_331292
Anti-rabbit IgG, HRP-linked Antibody	Cell Signaling Technology	Cat# 7074; RRID: AB_2099233
Anti-mouse IgG, HRP-linked Antibody	Cell Signaling Technology	Cat# 7076; RRID: AB_330924
Anti-UBP43 Rabbit pAb	Servicebio	Cat# GB111923
Bacterial and virus strains		
Lentiviruses containing miR-4769-3p mimics	GeneChem	N/A
Lentiviruses containing mimics NC	GeneChem	N/A
Lentiviruses containing USP18 siRNA (si-USP18)	GeneChem	N/A
Lentiviruses containing VDAC2 siRNA (si-VDAC2)	GeneChem	N/A
Lentiviruses containing si-NC	GeneChem	N/A
Lentiviruses containing VDAC2 overexpression plasmid (OE-VDAC2)	GeneChem	N/A
Lentiviruses containing OE-NC	GeneChem	N/A
Fusion vector carrying HA and USP18 (USP18-HA-OE)	RiboBio	N/A
Empty-vector	RiboBio	N/A
Biological samples		
Skin tissues	The Second Xiangya Hospital of Central South University	N/A
Plasma samples	The Second Xiangya Hospital of Central South University	N/A
Chemicals, peptides, and recombinant proteins		
Dexamethasone	Sigma-Aldrich	D4902
3-Isobutyl-1-methylxanthine (IBMX)	Sigma-Aldrich	I7018
Insulin	Abcam	ab123768
Oil Red O	Solarbio	G1260
Bleomycin	APExBIO	A8331
Lipofectamine™ 2000	Invitrogen	11668019
Polybrene	Beyotime	C0351
Puromycin	Sigma-Aldrich	540222
TRI Reagent	MRC	TR118

(*Continued on next page*)

Continued

REAGENT or RESOURCE	SOURCE	IDENTIFIER
Critical commercial assays		
Bulge-Loop™ miRNA qRT-PCR Starter Kit	RiboBio	C10211-2
RNA-FISH(miRNA) Kit	BersinBio	Bes1001
Hematoxylin–Eosin (H&E) Staining Kit	Solarbio	G1120
Modified Masson's Trichrome Stain Kit	Solarbio	G1346
riboFECT™ CP Transfection Kit	RiboBio	R10035.5
Evo M-MLV Reverse Transcription Kit	Accurate Biology	AG11706
SYBR® Green Pro Taq HS Premixed qPCR Kit	Accurate Biology	AG11701
GenSeq® ac4C RIP kit	CLOUD-SEQ	GS-ET-005
Dual Luciferase Reporter Gene Assay Kit	Yeasen	11402ES60
SuperSignal™ West Pico PLUS Chemiluminescent Substrate	Thermo Fisher Scientific	34580
Pierce™ Silver Stain for Mass Spectrometry	Thermo Fisher Scientific	24600
Experimental models: Cell lines		
3T3-L1 preadipocytes	Hunan Fenghui Biotechnology	N/A
Experimental models: Organisms/strains		
BALB/C mice	Hunan SJA Laboratory Animal Co., Ltd.	N/A
Oligonucleotides		
miR-4769-3p FISH probe: GTAGGGGAGGGAGGATGGCAGA	BersinBio	N/A
Antago-miR-4769-3p	RiboBio	N/A
Antago-NC	RiboBio	N/A
Bulge-Loop™ miRNA qRT-PCR Primer Sets (specific for miR-4769-3p)	RiboBio	N/A
USP18 Forward (5′ to 3′): AAGAGGAAGAGAGTGCTGTCTAG	This paper	N/A
USP18 Reverse (5′ to 3′): AGTTAAGGCAACACGTCTGTC	This paper	N/A
VDAC2 Forward (5′ to 3′): ACTCTGAGGCCTGGTGTGAAG	This paper	N/A
VDAC2 Reverse (5′ to 3′): CCAATTCCAAGGCAAGCCCA	This paper	N/A
GAPDH Forward (5′ to 3′): AGCCCAAGATGCCCTTCAGT	This paper	N/A
GAPDH Reverse (5′ to 3′): CCGTGTTCCTACCCCCAATG	This paper	N/A
Software and algorithms		
ImageJ	NIH	N/A
GraphPad Prism	GraphPad	N/A
Other		
Protein A/G Agarose Beads	Yeasen	36403ES08

RESOURCE AVAILABILITY

Lead contact

Further information and requests for resources and reagents should be directed to and will be fulfilled by the lead contact, Rong Xiao (xiaorong65@csu.edu.cn).

Materials availability

The study did not generate new unique reagents.

Data and code availability

- All data reported in this paper will be shared by the lead contact upon request.
- This paper does not report original code.
- Any additional information required to reanalyze the data reported in this paper is available from the lead contact upon request.

EXPERIMENTAL MODEL AND STUDY PARTICIPANT DETAILS

Clinical samples

Skin tissues were biopsied from the forearms of three SSc patients and three healthy donors, and plasma samples were obtained from 20 SSc patients and 20 healthy controls. All SSc patients enrolled in this study were first diagnosed at the Second Xiangya Hospital of Central South University, met the American College of Rheumatology criteria, and had never received systemic therapy, whereas patients with vascular or autoimmune diseases were excluded. All participants gave signed informed consent. This study was conducted in accordance with the principles of the Declaration of Helsinki and approved by the Ethics Committee of the Institutional Review Board of Central South University (approval ID: XR20211006).

Cell culture and induction of adipocyte differentiation

The 3T3-L1 preadipocytes were obtained from Hunan Fenghui Biotechnology (Changsha, China) and maintained in Dulbecco's Modified Eagle Medium (Thermo Fisher Scientific) containing 10% fetal bovine serum (Sigma-Aldrich) at 37°C with 5% CO_2. For adipocyte differentiation, confluent 3T3-L1 cells were cultured for an additional 2 days, and then treated with 1 μM dexamethasone (Sigma-Aldrich), 5 μg/mL insulin (Abcam), and 0.5 mM 3-isobutyl-1-methylxanthine (Sigma-Aldrich) in culture medium for 48 h. Next, the cells were treated with 5 μg/mL insulin in culture medium for another 48 h, and then cultured in complete medium, changed every 2 days, for an additional 8 days.

Animal model

Female BALB/C mice (weighing 18–22 g, aged 8 weeks) purchased from Hunan SJA Laboratory Animal Co., Ltd. (Changsha, China) were housed in specific pathogen-free conditions with a 12-h light-dark cycle, appropriate temperature and humidity, and adequate food and water. After 1 week of adaptive feeding, the mice were randomly divided into four groups: sham, BLM, BLM+Antago-NC, and BLM+Antago-miR-4769-3p (n = 5). All BLM groups received daily dorsal subcutaneous injections of bleomycin (200 μg/mL, APExBIO) for 4 weeks. Meanwhile, the sham group received dorsal subcutaneous injections of phosphate-buffered saline. For the next 4 weeks, mice in the BLM+Antago-miR-4769-3p group received weekly subcutaneous injection of Antago-miR-4769-3p (200 nM, RiboBio), and mice in the BLM+Antago-NC group received concurrent subcutaneous injection of Antago-NC (200 nM, RiboBio). No deaths were observed in any of the groups. All mice were euthanized by cervical dislocation, and skin tissues were collected for further experiments. The animal experiments were approved by the Animal Ethical Review Committee of Central South University (approval ID: CSU-2022-0001-0028).

METHOD DETAILS

RNA fluorescence *in situ* hybridization (RNA-FISH)

The expression of miR-4769-3p in skin samples was detected using an RNA-FISH(miRNA) kit (BersinBio) according to the manufacturer's instructions. Briefly, skin sections were deparaffinized and treated with protease. They were then hybridized overnight with a miR-4769-3p FISH probe (BersinBio) and observed by fluorescence microscopy after washing and staining with DAPI.

Hematoxylin–Eosin and Masson's staining

The obtained skin tissues were immersed in 4% paraformaldehyde, embedded in paraffin, and cut into 5-μm slices. To observe the pathological changes, skin sections were stained using the commercial Hematoxylin–Eosin (H&E) Staining Kit (Solarbio) and Modified Masson's Trichrome Stain Kit (Solarbio) according to the manufacturer's protocols and finally examined by light microscopy.

Immunohistochemical staining

The paraffin-embedded skin sections were subjected to deparaffinization and succeeding antigen retrieval with citrate buffer (pH 6.0). After incubation in 3% H_2O_2 for 10 min and blocking in 5% serum for 20 min, skin sections were incubated overnight at 4°C with primary antibodies against USP18 (also called UBP43, 1:1000, Servicebio) or VDAC2 (1:500, Proteintech) and then with HRP-linked secondary antibodies for 20 min. The positive staining was developed using diaminobenzidine solution and imaged under a light microscope.

Cell transfection and lentivirus infection

3T3-L1 cells were transfected with Antago-NC/Antago-miR-4769-3p (purchased from RiboBio) using a riboFECT CP Transfection Kit (RiboBio), and infected with Empty-vector/USP18-HA-OE (constructed by RiboBio) using Lipofectamine 2000 (Invitrogen). 3T3-L1 cells were infected with lentiviruses containing mimics NC/miR-4769-3p mimics, or si-NC/si-USP18/si-VDAC2, or OE-NC/OE-VDAC2 (packaged

by GeneChem) in the presence of 5 mg/mL polybrene (Beyotime), and positively infected cells were selected by treatment with 2 μg/mL puromycin (Sigma-Aldrich) for 1 week.

Quantitative real-time polymerase chain reaction (real-time qPCR)

Total RNA was extracted from 3T3-L1 cells/skin tissues using the TRI Reagent (MRC). The cDNA was synthesized using the Evo M-MLV Reverse Transcription Kit (Accurate Biology) and then amplified using the SYBR Green Pro Taq HS Premixed qPCR Kit (Accurate Biology). Gene expression normalized to GAPDH was calculated using the $2^{-\Delta\Delta Ct}$ method. miRNA quantification was determined using Bulge-Loop miRNA qRT-PCR Primer Sets (one RT primer and a pair of qPCR primers for each set) specific for miR-4769-3p (designed by RiboBio).

Oil Red O staining

To evaluate the lipid content after adipocyte differentiation, skin slides or 3T3-L1 cells fixed in 4% paraformaldehyde for 1 h were immersed in 60% isopropanol, then stained with Oil Red O solution (Solarbio) and observed under a light microscope.

RNA immunoprecipitation (RIP)

The GenSeq ac4C RIP kit (CLOUD-SEQ) was used to determine the binding between miR-4769-3p and USP18 according to the manufacturer's instructions. Briefly, 3T3-L1 cells were lysed with RIP lysis buffer and then immunoprecipitated with anti-Ago2 antibody (1:30, Abcam) and magnetic beads at 4°C overnight. After proteinase treatment, co-immunoprecipitated RNA was extracted, followed by reverse transcription, PCR, and 2% agarose gel electrophoresis of the PCR products.

Dual Luciferase reporter assay

To validate the binding of miR-4769-3p to USP18, the human or mouse USP18 3′UTR sequences containing wild-type or mutant miR-4769-3p binding sites were inserted into the pGL-3 vector. 3T3-L1 cells were co-transfected with these constructs together with miR-4769-3p mimics or mimics NC. After incubation for 24 h, luciferase activities were assayed using the Dual Luciferase Reporter Gene Assay Kit (Yeasen) according to the manufacturer's instructions.

Co-immunoprecipitation and mass spectrometry (coIP/MS)

Whole-cell extracts were obtained after lysis with Cell Immunoprecipitation Lysis Buffer. Protein samples were then incubated with A/G agarose beads for 2 h at 4°C, followed by overnight incubation with IgG (CST) and HA (Proteintech) at 4°C with rotation. After washing with lysis buffer, the immunoprecipitates were loaded with sodium dodecyl sulfate (SDS) loading buffer and boiled for subsequent analysis. For mass spectrometric analysis, protein samples were subjected to 10% SDS–polyacrylamide gels, followed by fixation, rinsing, immobilization sensitization, silver staining, and color development using the Pierce Silver Stain for Mass Spectrometry (Thermo Fisher Scientific). The collected protein bands were transferred for MS analysis by Shanghai Applied Protein Technology Co., Ltd. (China).

Western blot

Protein samples and immunoprecipitates extracted from 3T3-L1 cells/skin tissues were separated by SDS–polyacrylamide gel electrophoresis, electrophoretically transferred to polyvinylidene fluoride membranes, and blocked in 5% skim milk. Membranes were incubated overnight with primary antibodies against PPAR-γ (1:1,000, Abcam), FABP4 (1:1,000, Abcam), SREBP-1 (1:500, Abcam), Lipin1 (1:1,000, Abcam), USP18 (1:1,000, Proteintech), VDAC2 (1:1,000, Proteintech), HA (1:1,000, Proteintech), and Ubiquitin (1:1,000, CST) at 4°C. The membranes were then incubated with HRP-linked secondary antibodies (1:5,000, CST) for 1 h. Finally, the immunoreactive bands were detected using SuperSignal West Pico PLUS Chemiluminescent Substrate (Thermo Fisher Scientific), and protein expression normalized to GAPDH was calculated using ImageJ.

QUANTIFICATION AND STATISTICAL ANALYSIS

All statistical analyses were conducted using GraphPad Prism software. All data are reported as mean ± SEM. Three biological replicates were adopted for *in vitro* studies. Student's t test was used to analyze differences between experimental and control groups, and one-way analysis of variance (ANOVA) was used to analyze differences between multiple groups, with Tukey's post-hoc test. Statistical significance was considered at $p < 0.05$.